MATEC Web of Conferences **304**, 02004 (2019) https://doi.org/10.1051/matecconf/201930402004
EASN 2019

DESIGN AND INVESTIGATION OF FLAT-UPPER-SURFACE AIRFOIL

Cezary Galiński[1,*], *Magdalena* Gronowska[1], *Wieńczysław* Stalewski[2] and *Konrad* Gumowski[1]

[1]Warsaw University of Technology, Mechanical Faculty of Power and Aeronautical Engineering, ul. Nowowiejska 24, 00-665 Warszawa, Poland
[2]Sieć Badawcza Łukasiewicz – Instytut Lotnictwa, al. Krakowska 110/114, 02-256 Warszawa, Poland

Abstract. Attempts to build solar High Altitude Long Endurance (HALE) airplanes are more and more frequent. In the future such airplanes may appear very useful for the economy because they may replace geostationary satellites in several applications for a fraction of cost. Unfortunately, necessary data on altitude effect on photovoltaic cells and batteries performance are not easily available. Therefore, flying testbed for their inexpensive testing is needed. Flat-upper surface airfoil was designed for application in small UAV dedicated for photovoltaic cells investigation at various altitudes. It should enable installation of rigid cells on the top of the wing without significant reduction of aerodynamic performance. It should also decrease a risk of damage of flexible cells due to the significant bending of long aspect ratio, elastic wings. This paper contains description of the design methodology, design assumptions and obtained results. Moreover experiment undertaken to evaluate the design is described as well. The wind tunnel and a semi-span model used for this experiment are presented together with obtained results. The model has exactly the same structure as envisaged structure of UAV, so flexibility of the wing is taken into account.

1. Introduction

Interest in aeronautical electric propulsion systems has been growing for several years. It can be noticed in application of more numerous electric avionic systems instead of hydraulic and pneumatic [1]; in application of electric motors as propulsion of conventional airplanes [2] and in creation of new airplanes configurations [3]. These new types of airplanes could for example fly for many months at extremely high altitudes. As a result, they could work in the similar way as geostationary satellites [4] thus decreasing demand for them. This would be of particular importance for economy because of reduced service costs as well as for environment due to reduced number of space launchers take-offs. It would be also important from the operational point of view because the number of satellites on geostationary orbit is constrained. However, designers are facing some barriers making the task of very long endurance flights difficult or even impossible to perform. One of the most important is the lack of information on real characteristics of expensive devices that could be used in propulsion systems. Usually their published characteristics were obtained in the laboratory conditions at the sea level or on the level of laboratory where particular device was created. On the other hand application in real airplane requires information on real characteristics at different altitudes. Traditionally influence of the altitude was carefully studied in the case of internal combustion engines because of amount of oxygen available in ambient atmosphere on various altitudes for burning the fuel. Most of electric propulsions do not burn any fuels, therefore, they seem to be insensitive to the altitude. In reality they are exposed to the variation of pressure, temperature, radiation intensity and spectrum. Each of them may influence the efficiency of the propulsion. A few of these variations can be simulated on the ground [5] for example in the vacuum chamber, e.g. variation of ambient pressure and temperature. However, application of good vacuum chamber is usually quite expensive and does not allow for the simulation of radiation intensity and spectrum in full range experienced in the flight. These circumstances suggest that flight testing on the real airplane would be more useful. A few successful attempts to fly at high altitudes with solar electric propulsion have been already performed (Aerovironment Helios [6], Quinetic Zephyr [7]) as well as attempts to fly with very long endurance (Solar Impulse [8]). Unfortunately, these airplanes were quite large and expensive. In the contrary the airplane for photovoltaic cells testing at high altitudes should be inexpensive, so also small and simple in operations. The weight of such an experimental UAV could be minimized because long endurance would not be required, so heavy load of lithium batteries is also not necessary. Preliminary study on such an airplane was presented in [9]. In general it proved possibility of such an experiment, however, it also raised several significant questions. Wings of this UAV should allow for installation of various types of photovoltaic cells including rigid ones. Therefore it would be advantageous to apply an airfoil with as large as possible flat-upper-surface. Flat-upper-surface would be also useful in the case of flexible cells since they usually tolerate deflection only in one direction. Attempt to bend the cell in two directions simultaneously may result in the permanent damage. Unfortunately high altitude airplanes have to be very light. Moreover, they need wings with very long aspect ratio. As a result significant bending can be expected along the wing span [10-12]. This bending could destroy cells previously bended along the wing chord in order to follow the shape of an airfoil. Unfortunately airfoils with flat upper surface are not frequently present in airfoils catalogues [e.g. 13-15]. Therefore an attempt was undertaken to design an airfoil with 75% of its upper surface flat. The research was focused on maximization of lift to drag ratio and power factor, assuming low Reynolds numbers conditions since it was designed for small UAV.

2. Methodology

The design and optimisation of flat-upper-surface airfoil was conducted with the use of the following computational tools:
CODA4W - in-house code supporting airfoil design. The software is a very convenient interactive tool when designing airfoils. It is equipped with several modules. Among the others they are responsible for a precise controlling of smoothness of designed curves as well as simple analysis of flow around a designed airfoil. It was previously applied in several other projects [16, 17].
INVDES - in-house code solving the inverse-airfoil-design problem. The software enables to design a shape of the airfoil realizing defined distribution of pressure (or tangential velocity) in flow at given angle of attack. The definition of the required pressure distribution is conducted using a convenient Graphical User Interface. Apart of pressure definition, the user defines parts of airfoil which are allowed to be modified and the part that should be frozen. It was also previously applied in several other projects [16, 17].
XFLR-5 [18] - commonly used code for aerodynamic analysis of airfoils and wings in low-speed conditions. The program is widely recognized as one of the best in model-scale-aircraft aerodynamics. For given Reynolds and Mach number, the software enables to determine all

basic aerodynamic characteristics of the airfoil also within the range of critical angles of attack, where the maximum lift coefficient is reached.
A18 airfoil [9] was chosen as a starting point. It was successfully applied in free flying FAI models, so it was assumed that its low Reynolds number performance is superior. Its upper surface was then modified. Aft part was replaced by the straight line parallel to the tangent to the lower siluethe at the trailing edge. As a result trailing edge was acceptable from manufacturing point of view. Then front part was added in such a way that it was tangent to the trailing straight line in 25% of the chord. This new airfoil A18FT4 was taken as a baseline for the further development. Within the process, this baseline airfoil was modified, mainly through a redesigning its shape except the fixed flat part of its upper surface. So, the design was focused on redesigning of nose part of the airfoil as well as its lower surface.
Aerodynamic characteristics of designed variants of the airfoil, were determined using the XFLR-5 software.
Instead of ineffective "trial-and-error" approach, the approach based on sensitivity analysis was applied. In this approach several design parameters defining airfoil shape, were taken into account, and the design process was conducted based on analysis of an influence of these parameters on aerodynamic characteristics of the airfoil, including lift-over-drag ratio - the main criterion of the airfoil designing. While the flat part of the airfoil was fixed, the design parameters defined vertical position of the leading edge and influenced the curvature distribution of the front part of the airfoil.

3. Design of the Airfoil

According to [9] experimental UAV should have optimal airspeed equal to 8 m/s at the sea level. This airspeed was assumed as the most important because of safety of the flight at low altitude with small climb rate. Therefore attention was put at the following flight conditions:

Altitude: Sea Level ISA
Velocity: V= 8 m/s
Temperature: T = 288.15 K
Mach number: M = 0.0235
Reynolds number: Re = $92*10^3$

In the initial stage of the design process, the aerodynamic properties of the baseline airfoil A18FT4 were analysed. The aerodynamic characteristics of the A18FT4 airfoil were calculated using the XFLR-5 code. In these calculations, the natural laminar-to-turbulent transition as well as forced transition at various chord percentages, was investigated. Selected results of these calculations are presented in Figure 1. It is visible from this plot that the C_L/C_D is higher for the cases corresponding to forced transition than for the Natural Laminar Flow on the upper surface of the airfoil for assumed design point. This observation is not surprising for so small Reynolds numbers [15]. Searching for the optimal chordwise position of the forced transition led to the choice of the transition point at 19% of chord. Similar study conducted with respect to the lower surface of the airfoil, led to the conclusion that on the lower surface Natural Laminar Flow (no forced transition) favours the highest lift-over-drag ratios.

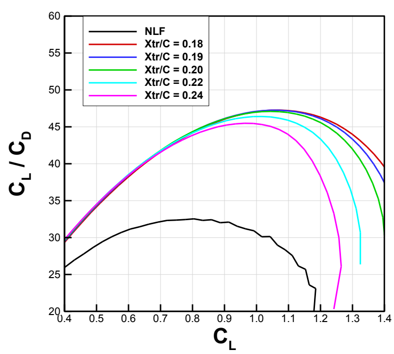

Fig. 1. Lift-over-drag ratio (C_L/C_D) versus lift coefficient (C_L), for Natural Laminar Flow (NLF) on the upper surface as well as for the forced laminar-to-turbulent transition on upper the surface, at 18%, 19%, 20%, 22% and 24% of airfoil chord. Results of computations conducted for the airfoil A18FT4

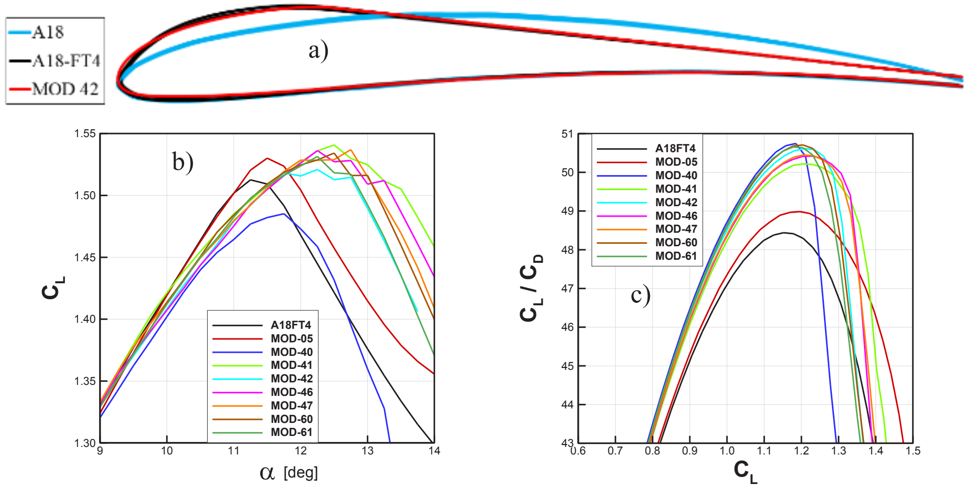

Fig. 2. a) Shapes of original A18, baseline A18FT4 and finally chosen MOD-42 airfoils; b) Lift coefficient (C_L) versus angle of attack (α), for the baseline A18FT4 and selected airfoils - results of design process; c) Lift-over-drag ratio (C_L/C_D) versus lift coefficient (C_L), for the baseline A18FT4 and selected airfoils - results of the design process

Based on results of the above calculations, the additional design parameter was introduced. It was the chord percentage of forced laminar-to-turbulent transition on an upper surface of the airfoil. During the design process, this parameter was selected separately for each designed airfoil. However, in most cases the optimal position of forced transition was obtained also at about 19% of airfoil chord. On the lower surface, the natural laminar-to-turbulent transition was assumed for all designed airfoils.
During the design and optimisation process more than 80 different airfoils were designed and investigated computationally. Finally chosen airfoil is presented in Figure 2a, compared with baseline and original A18 airfolis.
Many from the designed airfoils were obtained as results of solution of inverse problem. Additionally, sequences of airfoils were obtained through systematic changes of selected design parameters (e.g. vertical position of a leading edge of the wing).

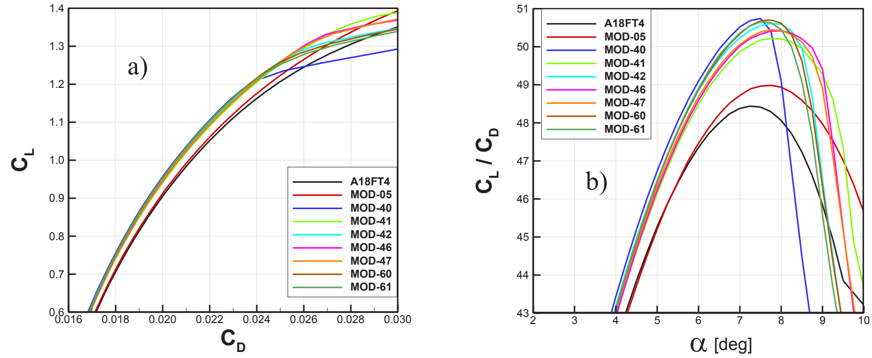

Fig. 3. a) Lift coefficient (C_L) versus drag coefficient (C_D), for the baseline A18FT4 and selected airfoils - results of the design process; b) Lift-over-drag ratio (C_L/C_D) versus angle of attack (α), for the baseline A18FT4 and selected airfoils - results of the design process

Figure 2c compares dependencies: lift-over-drag ratio (C_L/C_D) versus lift coefficient (C_L), for the baseline A18FT4 and selected airfoils. All selected modifications, except the MOD-05,

indicate visible higher lift-over-drag ratio than the baseline A18FT4. Figure 3a compares drag polars calculated for the baseline A18FT4 and selected airfoils. Nearly all airfoils, except the MOD-05 and MOD-40 (for C_L>1.2), are characterised by significantly more favourable drag polars than the baseline. All new airfoils can be divided into four groups. MOD-05 is only slightly better than the baseline. MOD-40, MOD-60 and MOD-61 have the best maximal value of lift-over-drag ratio, but their best performance exist in the narrow range of angles of attack. MOD-41, MOD-46 and MOD-47 have significantly lower maximal value of lift-over-drag ratio, but they also have better performance at high angles of attack than airfoils from the previous group. Performance of MOD-42 look like a kind of compromise. Its maximal value of lift-over-drag ratio is slightly smaller than in the case of airfoils from the second group, but better than in the case of airfoils from the third group. Moreover its high lift performance is better than in the case of airfoils from the second group. That is why this airfoil was selected for further investigation, although the other airfoils are not much worse. Figure 2a shows dependency of lift coefficient versus angle of attack. In the case of selected airfoil maximal value of the lift coefficient is smaller than in the case of most of analysed airfoils. However extremely slow flight capability was not required so relatively small $C_L$max was not considered as a significant drawback.
The finally selected airfoil MOD-42, compared to the baseline A18FT4, is characterised by:

- higher by 1.0÷2.0 lift-over-drag ratio, within the C_L range: $0.9 \leq CL \leq 1.3$,
- maximum lift coefficient higher by 0.01,
- delayed deep stall.

4. Wind tunnel experiment

Selected airfoil was used to build a wind tunnel model of the UAV wing. Measurement of the final wing design performance was a main goal of the experiment rather than verification of calculations. Moreover achievable weight of the wing structure was also very interesting. That is why the model was built with application of lightweight structure, not typical for wind tunnel models. This assumption decreased accuracy of the model shape, however allowed to obtain more realistic wind tunnel data. Among others they included the effect of the wing flexibility, which is important in the case of light wings with long aspect ratio.

4.1. Description of the model structure

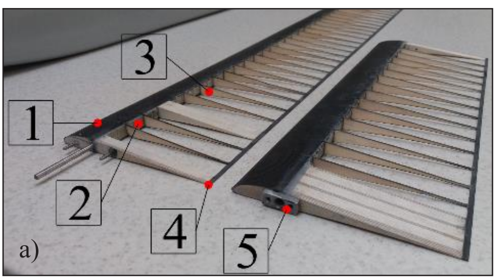

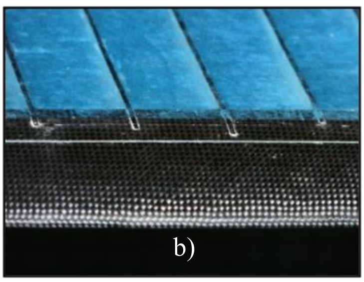

Fig. 4. a) Elements of the model structure. 1 – wing D-box, 2 – spar, 3 – balsa ribs, 4 – trailing edge, 5 – adapter. b) Elastic skin (blue surface) and turbulator (white line) at 19% of chord.

Model of the wing was built as a semi-span model, divided into two parts: center wing and wingtip. Center wing has the chord length equal to 0.17m and semispan of 0.5m. Wingtip has the chord length equal to 0.17m and semispan of 1m. So altogether the semispan of the complete model is equal to 1.5m. As it is shown in Figure 4 skin of the wing D-box (1) is made from carbon fabric. Inside there are balsa ribs, reinforcing the structure and preventing the D-box skin from buckling. Spar has unidirectional carbon caps and balsa wood shear web (2) reinforced with kevlar fibres. Geometry of the wing alongside wingspan is provided by balsa ribs (3). In order to increase their strength and rigidity ribs are supported with carbon fibres. Their number results from need to support wing elastic skin (see Fig. 4b). Trailing edge is also made from unidirectional carbon batten (4). Adapter (5) is an interconnection between the model and the aerodynamic balance. Complete weight of the model is 240g. In the final design this weight could be decreased because adapter would not be necessary.

4.2 Description of the wind tunnel

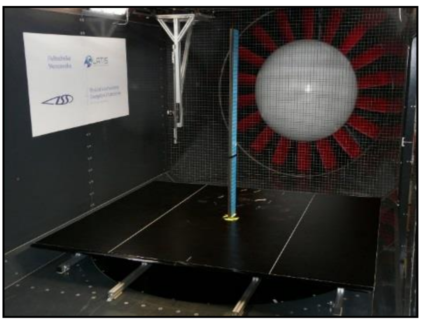

Fig. 5. The test stand with mounted model of the wing inside the wind tunnel

Model was tested in the low speed wind tunnel owned by Warsaw University of Technology, in the measurement section characterised by width of 2,5m and height of 2,1m. Stream velocities from 6m/s to 25m/s are available in this measurement section. The turbulence level is smaller than 4% in applied velocity range.

Measurements were conducted on the test stand designed specifically for researching different types of semi-span models [19]. Stand is equipped with separation table, responsible for neutralizing effects of boundary layer. Rotating section of the wind tunnel floor, located underneath the table, allows to change the angle of attack. The aerodynamic balance is also attached to this rotating floor. Forces and moments are transferred to the balance, through pin - adapter connection. The pin extends above the separation table allowing for installation of the model slightly above the separation table. Measurements results are recorded and post-processed by in-house build data acquisition system based on LabView platform with 24bit A/D converter.

4.3 Measurements results

Research program included four configurations:

Table 1. Research program.

Configuration	Parts	α [°]	V [m/s]
Smooth airfoil	center wing only	-5 ÷ 20	6 ÷ 14
	full aspect ratio		6 ÷ 10
Airfoil with turbulator at 19% of chord	center wing only		6 ÷ 14
	full aspect ratio		6 ÷ 10

Limit of velocity for full aspect ratio configuration results from constrained strength and large deflections of the wing. Higher loads from increased air speeds in the tunnel could result in damage of the test model. On the other hand real airplane will never fly with maximum airseed at high angles of attack so full range of airspeeds and angles of attack was not necessary. Therefore the effect of Reynolds number variation was more thoroughly investigated only for the center-wing.

In case of the center wing with turbulator lift coefficient is slightly higher than for smooth one. Difference in values of maximum lift coefficient is 0,037. This variation is even lesser in the case of full aspect ratio. All configurations have equally smooth stall and their critical angle of attack equals 14,6°. Maximum obtained lift coefficient C_L = 1,238 was achieved for full aspect ratio with turbulator.

In both configurations with turbulator drag characteristics are relocated towards smaller drag in comparison to smooth configurations. For full aspect ratio (Fig. 6b) there is a behaviour of holding smaller drag coefficient values for wider range of lift coefficients. The center wing configuration characteristics keep being similar with and without turbulator and is only shifted. Minimum obtained drag coefficient C_D = 0,018 is obtained for full aspect ratio.

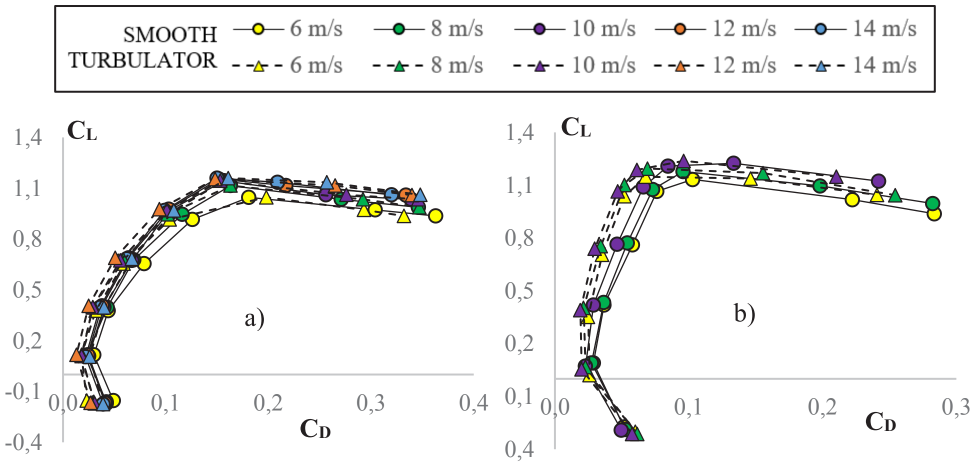

Fig. 6. Lift coefficient (C_L) versus drag coefficient (C_D), in two configurations: smooth airfoil and with turbulator for a) wing center and b) full aspect ratio

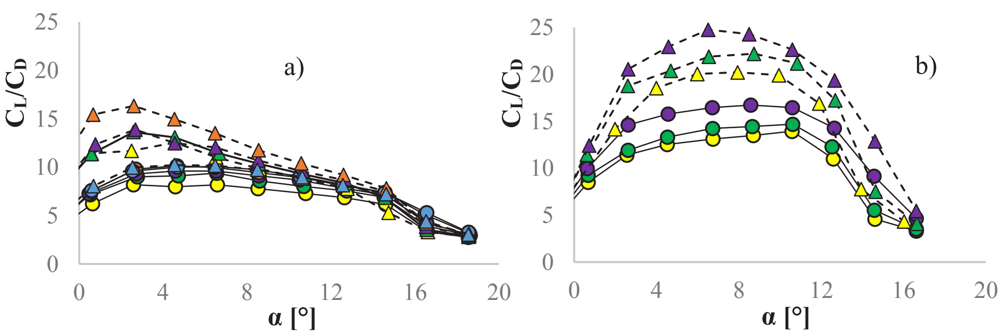

Fig. 7: Lift-over-drag ratio (C_L/C_D) versus angle of attack (α), in two configurations: smooth airfoil and with turbulator for a) wing center and b) full aspect ratio

In both configurations, of center wing and full aspect ratio, turbulator provides meaningful growth of C_L/C_D values. Greatest difference occurs for full aspect ratio with 12 m/s velocity. Smooth configuration has C_L/C_D equal to 16.4 while configuration with turbulator has 24.8. Although, for 14 m/s velocity the effect of forced transition disappears on the center-wing and curve becomes similar to smooth configuration.

Values of C_L/C_D obtained from this wind tunnel experiment are close to values expected for the wing with original A18 airfoil. Therefore it seems like the airfoil with flat-upper-surface is not worse than the original one.

5 Conclusion

Airfoil with flat-upper-surface was designed. It was used to build lightweight wind tunnel model with flexibility similar to the flexibility of the final UAV wing design. Then the model was investigated in the wind tunnel revealing satisfactory characteristics.
Lift over drag ratio appeared better for the model with turbulator installed then for the model without turbulator. This phenomenon frequently occurs at low Reynolds numbers. The greatest advantage was achieved when turbulator was installed at 19% of the chord on the upper surface of the wing

References

1. J.A. Rosero, J.A. Ortega, E. Aldabas, IEEE A&E Systems Magazine, Vo. 22, No 3, 2007, pp. 3-9
2. B. Łukasik, W. Wiśniowski, Journal of KONES Powertrain and Transport, Vol. 23, No. 4, 2016, pp. 305-310.
3. S. Stuckl, J. van Toor, H. Lobentanzer, proceedings of 28th ICAS conference, Brisbane, Australia, 23-28 September 2012
4. J. Gavan, S. Tapuchi, D. Grace, Radio Science Bulletin, No 330, September 2009, pp. 20-31.
5. Z. Jakielaszek, M. Nowakowski, Journal of KONES Powertrain and Transport, Vol. 21, No. 4, 2014, pp.203-210.
6. Y. Gibbs, https://www.nasa.gov/centers/armstrong/news/FactSheets/FS-068-DFRC.html, NASA web page seen on 25.07.2018.
7. J. Amos, BBC News, 16 July 2010.
8. H. Ross, AIAA/ICAS conference paper 129913, Anchorage, USA, September 2008.
9. C. Galinski, Journal of KONES Powertrain and Transport, Vol. 25, No. 3, 2018, pp. 167-174.
10. Z. Goraj, T. Ueda, proceedings of 22th ICAS conference, Harrogate, UK, 27 August-1 September 2000.
11. C. Min, Z. Zhou, W. Rui, X. Xiaoping, proceedings of 29th ICAS conference, St. Petersburg, Russia, 7-12 September 2014.
12. G. Romeo, G. Frulla, E. Cestino, Proceedings of the Institution of Mechanical Engineers, Part G: Journal of Aerospace Engineering, pp.199-216.
13. I.H. Abbot, A.E. von Denhoff, Dover Publications, inc., New York, 1959
14. D. Althaus, F.X. Wortmann, Friedr. Vieweg&Sohn Verlagsgesellschaft mbH, Braunschweig, 1981
15. C.A. Lyon, A.P. Broeren, P. Giguere, A. Gopalarathnam, M.S. Selig, SoarTech Publications, Virginia Beach, VA, 1998.
16. W. Stalewski, Journal of KONES Powertrain and Transport, Vol. 24, No. 4, 2017, pp. 287-295.
17. W. Stalewski, W. Zalewski, Journal of KONES Powertrain and Transport, Vol. 22, No. 2, 2015, pp. 221-232.
18. M. Drella, H. Youngren, M. Scherrer, A. Deperrois, XFLR-5, 2012. available at: http://www.xflr5.com/xflr5.htm
19. T. Banaszek – Master thesis in polish. Not published, Warszawa, 2018